

Paromomycin-Loaded Mannosylated Chitosan Nanoparticles: Targeted Drug Delivery Against BALB/c Mice Infected To *L.Major*

Farideh Esfandiari

Shiraz University of Medical Sciences

Hossein Heli

Shiraz University of Medical Sciences

Qasem Asgari

Shiraz University of Medical Sciences

Mohammad Hossein Morowvat

Shiraz University of Medical Sciences

Afshin Barazesh

Shiraz University of Medical Sciences

Fatemeh Goudarzi

Shiraz University of Medical Sciences

Neda Pirbonyeh

Shiraz University of Medical Sciences

Mohammad Motazedian (✉ motazedm@sums.ac.ir)

Shiraz University of Medical Sciences

Research

Keywords: Paromomycin, Mannosylation, qPCR, Leishmaniasis, L.major

Posted Date: June 16th, 2021

DOI: <https://doi.org/10.21203/rs.3.rs-291994/v1>

License: © ⓘ This work is licensed under a Creative Commons Attribution 4.0 International License.

[Read Full License](#)

Abstract

Cutaneous leishmaniasis (CL) is a disease with unsatisfactory current therapies due to the emergence of drug resistance and toxicity. Paromomycin (PM), though recently have received more attention for its anti-*Leishmania* activity, suffers from poor oral bioavailability, limited efficacy and rapid clearance in parenteral route. In this study, we examined the efficacy of nanoparticle-based PM delivery system in treating the murine model infected with *Leishmania major* (*L. major*). Paromomycin was loaded in mannosylated chitosan-dextran nanoparticles (PM-MCS-dex-NPs) through ionic gelation method. The particle size and zeta potential of PM-MCS-dex-NPs were obtained as 246 nm and +31 mV, respectively. PM-MCS-dex-NPs effectively affected both stages of the parasite especially the amastigote one in vitro culture. Nanoformulation injected intramuscularly into mice for up to 21 days. Lesion sizes were measured before the onset of treatment and at weekly intervals for a month. In addition, the DNA copy number was quantified in the infected mice by a real time quantitative polymerase chain reaction (qPCR). *In vivo* results showed that the administration of PM-MCS-dex-NPs with a dose of 10 mg/kg/twice daily significantly reduced the lesion size and DNA copy number compared to the other treatment methods. Lesions sizes in both control groups of chitosan nanoparticles (CS-NPs) and mannosylated nanoparticles (MCS-NPs) were also significantly ($p < 0.05$) decreased in comparison with the untreated control, suggesting the wound healing property of chitosan. PM-MCS-dex-NPs proved as a promising candidate in delivering PM by boosting the drug solubility and targeting the infected macrophage cells. The results of this study can provide a new and efficient drug delivery system for CL treatment.

Highlights

- Paromomycin was loaded into chitosan nanoparticles with a high efficiency using an ionic gelation method.
- PM-MCS-dex-NPs were administrated twice a day in mice.
- PM-MCS-dex-NPs illustrated a significant therapeutic efficacy, compared to free PM or glucantim

Introduction

Leishmaniasis is a parasitic disease caused by Trypanosomatidae family and transmitted by phlebotomine sandflies. It manifests in three main forms, effecting people mainly in the developing countries (Alvar et al., 2012; Torres-Guerrero et al., 2017; Bocxlaer et al., 2019). World Health Organization (WHO) estimates that annually about 1.2 million cases of cutaneous leishmaniasis (CL) and 500,000 cases of visceral leishmaniasis (VL) become lethal if they remain untreated. Regarding treatment, chemotherapy is the primary method to control leishmaniasis (Savioli and Daumeric, 2010); however, the occurrence of drug resistance in disease-endemic countries, drug toxicity, needing long-term treatment period and disease relapse are the most important impediments in treating leishmaniasis (Croft et al., 2006; Kedzierski et al., 2009; Yasinzai et al., 2013; Ponte-Sucre et al., 2017). Among conventional drugs, pentavalent antimonials, as the first choice drugs for the treatment of leishmaniasis, encountered

resistance and serious side effects in majority of the developing countries, which led to limiting their usage (Al-Natour, 2009; Gomez Perez et al., 2016; Eddaikra et al., 2018). The second line of drugs, including Amphotericin B (AmB), pentamidine and miltefosine are less popular due to their high cost, side effects and the need for hospitalization (Mohapatra, 2014). Among the second line drugs, paromomycin (PM) (also known as aminosidine) has lower cost, is more accessible, and has fewer side-effects. PM is an aminoglycoside antibiotic active against *Leishmania* parasite with no teratogenic properties (Sinha et al., 2011). Anti leishmania effects of PM has been reported since 1960s and since then, it has been used in several clinical trials targeting leishmaniasis (Croft and Yardley, 2002).

While it remains largely unclear, various mechanisms of action have been suggested for PM in *Leishmania*. Some reports have suggested that the cationic property of paromomycin leads its binding to leishmanial glycolyx and lipophosphoglycan holding negative charge property (Chawla et al., 2011; Jhingran et al., 2009). Another report has pointed to the blocking of mRNA translation by binding to 30S subunit of ribosome. (Maarouf et al., 1995; Sundar and Chakravarty, 2008).

Despite its promising benefits, PM suffers from poor absorption into systemic circulation after oral administration, low penetration through the stratum corneum of the skin after local administration and rapid clearance from circulating system upon parenteral injection. Overcoming such issues and improving the efficacy of PM can be addressed by nanotechnology driven drug delivery systems. Different approaches with new nanoformulations including lipid based nanoparticles; liposome (Bavarsad et al., 2012; Carneiro et al., 2010; Ferreira et al., 2004; kalantari et al., 2014), Solid lipid nanoparticles (Ghadiri et al., 2011) and nanogel formulation (Brugues et al., 2015) have been proposed that can be used for PM delivery. In this study, we addressed these limitations using nanotechnology and targeted therapy.

Since *Leishmania* parasites reside mainly in the phagolysosome of the infected macrophage, new formulations which can enhance the drug delivery into the infected macrophages are of high interest. Cell surface expression of mannose receptor in macrophages has been used to facilitate the drug delivery. The receptor can recognize terminal mannose found on the surface of the pathogens, and plays a role in the uptake of the pathogen. Taking advantage of this property, Mannosylation of nanoparticles have shown to enhance its entry into the macrophage cells (Chellat et al., 2005).

Here, we examined the ability of paromomycin loaded on a new formulation based on chitosan mannosylated nanoparticles to target macrophages and evaluated the effect of this formulation on experimentally infected BALB/c mice with *L. major*.

Material And Methods

2.1. Chemicals

To fulfill the aim of the study, the following materials were provided. PM sulfate was obtained from MedChem Express (Shanghai, China) and Chitosan (CS) of average molecular weight of 120 kDa (with a

degree of deacetylation of 75–85%) was acquired from Sigma (St. Louis, MO). Also, Glucantim was purchased from Cipla Ltd. (Mumbai, India) and Sodium triacetoxymethylborohydride, (TPP) from Scharlau (Barcelona, Spain). RPMI-1640, fetal calf serum (FCS) and penicillin/streptomycin were both obtained from Sigma (St. Louis, MO). Agarose gel was purchased from SYBR safe stain (YTA, Iran) and Glacial acetic acid was received from Merck (Darmstadt, Germany). Finally, a punch biopsy was obtained from Kai medical (Oyana, Japan).

2.2. Ethical statement

The animal care and the experimental protocols were approved by the Institutional Animal Care and Research Advisory Committee at the Shiraz University of Medical Sciences (IR.SUMS.REC.1396.S375).

2.3. Syntheses of PM-MCS-dex-NPs

In order to synthesize PM-MCS-dex-NPs, the procedure used by Esfandiari et al. was followed (Esfandiari et al., 2019). First, MCS solution was made (0.2% w/v) by using acetic acid (0.1% w/v) and adjusting pH to 4.8. Then, PM (0.2% w/v) and dextran sulfate (0.12% w/v) solutions which had equal volumes were well mixed and added to MCS solution. In order to make the gelation solution, TPP solution (0.08% w/v) was made with pH of 5 and gradually added to the previous solution by using an insulin syringe under magnetic stirring at 800rpm for 30 min. Afterwards, the current suspension was sonicated at a power of 100 W and a frequency of 30 kHz for 10 min. The content was then stirred at 800 rpm at room temperature for about 20 min. By ultracentrifugation at 40000 rpm and 15 °C for 30 min. The particles were collected and dialyzed for the removal of the free drug. Afterwards, the formulation was freeze dried to obtain a dry powder of the nanoparticles and then stored at 4 °C. The final step was freeze-drying the formulation and storing the obtained dry powder at 4 °C. PM-CS-dex-NPs were prepared following a similar procedure. The only difference was that CS was used instead of MCS.

2.4. Parasite cultivation

L. major standard strain (MRHO/IR/75/ER) promastigotes were obtained from infected BALB/c mice tail base, grown in culture NNN medium and sub-cultured in RPMI-1640 medium supplemented with 12% (v/v) heat-inactivated FCS, 100 U mL⁻¹ penicillin and 100 µg mL⁻¹ streptomycin.

2.5. Animal handling

Fifty five female BALB/c mice (4–6 weeks old) weighing approximately 22g were purchased from Pasteur Institute (Iran). The animal care and the experimental protocols were approved by the Institutional Animal Care and Research Advisory Committee at Shiraz University of Medical Sciences (1396.S375). The animals were housed in standard cages under stable conditions (humidity 60–70%, temperature 25 ± 3°C, and 12:12-h dark-light cycles). 100 µL of 5×10³ cell/ml *L. major* amastigotes from infected BALB/c mice was injected subcutaneously in the mice tail base. After 4 weeks, nodules and ulcers were exhibited. The mice were randomly divided into 11 groups of five members. Before initiating

the treatment, each lesion area was achieved by a caliper through measuring two diameters of “a” and “b” with calculating ellipse area formula, where “a” and “b” were the smallest and largest diameters, respectively, using the following formula:

$$\text{Lesion size area (LS)} = (a/2 \times b/2) \times 3.14 \quad (1)$$

, 0.1 mL of the formulations was intramuscularly injected to all groups for 21 days. Table 1 illustrates the groups and doses formulations. At the end of each week, the lesions size was measured.

Table 1
Doses of drug administration in different mice groups.

Group	Formulation	Dose / mg kg ⁻¹
G1	Free PM	20
G2	PM-CS-dex-NPs	10
G3	PM-CS-dex-NPs	20
G4	PM-MCS-dex-NPs	5
G5	PM-MCS-dex-NPs	10
G6	PM-MCS-dex-NPs	20
G7	PM-MCS-dex-NPs*	10
G8	CS-NPs	20
G9	MCS-NPs	20
G10	PBS	-
G11	Glucantim	20
*Twice a day		

2.6. Punch biopsy

One week after the treatment completion, 2-mm diameter punch biopsies from the ulcer margins were removed in all groups, using a skin punch biopsy preserved at -20°C until further analysis.

2.7. Sample preparation for DNA extraction

DNA was extracted from skin biopsy specimens according to the manufacturer’s protocol, using QiAmp DNA Mini extraction kit from Qiagen (Valencia, California). Firstly, proteinases K was added to the skin biopsies. Then, were incubated for 60 min at 60°C and for 10 min at 70°C. The remaining steps were followed according to the manufacturer’s instructions by adding ethanol absolute into the samples and

transferring them to the kit columns. Also nucleic acid purity assessment was performed by a NanoDrop Instrument called Thermo Scientific™ 2000 (Wilmington, USA).

2.8. Construct of a standard curve for DNA quantitation

In order to prepare a standard curve, DNA extraction from 2×10^6 *L. major* promastigotes was carried out using a DNA isolation Kit from Favorgen Biotech (Pingtung, Taiwan) according to its manufacturer's protocol. The primers of LIN4R (forward: 5'-GGGGTTGGTGTAAAATAGGG-3') and LIN17 (reverse: 5'-TTTGAACGGGATTTCTG-3') were used for PCR analysis of the purified DNA. PCR products were analyzed by 1.5% neutral agarose gels electrophoresis. The gels were visualized under UV light with a transilluminator of UVT-20M from KIAGEN TEB Sadra (Tehran, Iran), and the bands were cut with a razor blade. Nucleic acid concentration was measured by the NanoDrop Instrument Thermo Scientific™ 2000 (Wilmington, USA). Then, copy number of *L. major* template DNA was calculated based on the following formula:

$$\text{Number of copies (molecules)} = [X (\text{ng}) \times 6.022 \times 10^{23}] / [\text{length (bp)} \times \text{conversion factor} \times 660] \quad (2)$$

Where X is the amount of DNA in the sample, 6.022×10^{23} is the Avogadro's constant, length is the base pairs (bp) of the DNA template, the conversion factor equals to 1×10^9 , and the average mass of 1 bp of dsDNA is 660 g mol^{-1} . For standardization of qPCR detection assay, ten-fold dilution series of the *L. major* genomic DNA was applied to construct a six-point calibration plot of cycle threshold (Ct) values versus DNA copy numbers.

2.9. DNA quantitation in lesion samples by qPCR

DNA quantitation by qPCR technique was established based on the amplification of *L. major* minicircle DNA to estimate the copy number of parasite in the BALB/c mice skin biopsies. Amplification was performed in a 25 μL reaction mixture containing 2 μL of the extracted genomic DNA, 10 μM of each primer targeting the kinetoplastid minicircle regions RV1 and RV2 (Forward: 5'-CTTTTCTGGTCCCGCGGGTAGG-3'; Reverse: 5'-CCACCTGGCCTATTTTACACCA-3' (Khadir et al., 2018), and 1X of 2X Quanti Fast SYBR Green master mix (Qiagen, Germany) with Diethylpyrocarbonate (DEPC) water brought to final volume following thermal cycling protocol. One cycle of primary for 5 min at 95°C, followed by 40 cycles of 15 s at 95°C denaturation, one min at 63°C, and 40 s at 72°C. Negative controls were included in order to confirm specificity and to assess the contamination rate of the primers. After preparing the reaction mixtures in reaction tubes, the tubes were mini spin centrifuged. Amplification and detection were performed with Quant3studio qPCR system.

2.10. Statistical analysis

Statistical analysis was performed using the SPSS (version 25) software. The difference between the lesion sizes in different groups during treatment was performed by repeated measures one-way ANOVA analysis followed by the Tukey post hoc test. The p value < 0.05 was considered statistically significant.

Results

3.1. Characterization of PM-CS-dex-NPs

PM-CS-dex-NPs were synthesized and characterized as reported in our previous study (Esfandiari et al., 2019). PM-MCS-dex-NPs had a particle size of 246 nm, zeta potential of + 31 mV and encapsulation efficacy of 83.5%, with a mannosylation level of 17% (w). *In vitro* culture in previous (Esfandiari et al., 2019) study, half-maximal inhibitory concentration values toward the THP-1 cells for PM aqueous solution and PM-MCS-dex-NPs after 48 h were obtained as 1846 ± 158 , and $2714 \pm 126 \mu\text{g mL}^{-1}$, respectively. Half – maximal inhibitory concentration values toward the promastigotes for PM aqueous solution and PM-MCS-dex-NPs after 48 h were obtained as 105.0 ± 14.0 and $17.8 \pm 1.0 \mu\text{g mL}^{-1}$, respectively. The parasite burden in THP-1 cells after 48 h treatment with PM aqueous solution and PM-MCS-dex-NPs at a typical concentration of $20 \mu\text{g mL}^{-1}$ were 71.78 and 33.41%, respectively.

3.2. Lesion size measurement

In all groups, the mice survived with zero mortality rate at the end of study. There were no significant differences ($p > 0.05$) in the lesion sizes among different groups at the beginning (week 0) until the second week of treatment. In week 3 and 4 of treatment, the lesion size was reduced ($p < 0.05$) significantly in G7 as compared to the other groups. The mean \pm SD lesion size one week after treatment in G7 was $11.02 \pm 2.4 \text{mm}^2$, whereas it was 80.5 ± 10 and $49.9 \pm 6.7 \text{mm}^2$ in G10 and G11, respectively. On the other hand, the lesion size of two groups PM-CS-dex-NPs and PM-MCS-dex-NPs in 10 and 20 mg kg^{-1} concentrations were significantly ($p < 0.05$) different. Lesions size in both control groups of G8 and G9 significantly ($p < 0.05$) decreased in comparison with the G10. Also, statistical analysis of the mean \pm SD showed significant difference between G7 with G11 and G1 with $p = 0.001$ and $p = 0.04$, respectively. Besides, increase in dose of formulations caused decline in the level of lesions size. Moreover, reduction in the lesion size in G7 happened faster than when formulations were used without mannose. Compared to G10, G8 and G9 had significant ($p < 0.05$) effect on the mice wound healing. The progressive increase was seen in lesion size of G10 with bacterial infection in the lesion site. These results suggest that the bactericidal action of chitosan was induced in both groups. The results revealed that the administration of (10 mg/kg) of PM-MCS-dex-NPs twice a day had the maximum effect on decline in the lesions size.

3.3. Standard curve for qPCR

The results of a standard curve for copy number determination by qPCR is demonstrated in Fig. 2. This curve was linear with a slope of -3.36, an intercept of 2.83, and R^2 value of 0.999.

3.4. Copy number determination in biopsy of lesions

Melting curves of SYBR green qPCR products are shown in (Fig. 3). One week after the end of treatment, *L. major* DNA copy number was evaluated in the skin lesions of all mice groups by qPCR as presented in Table 2. The mice treated by PM-MCS-dex-NPs showed significantly ($p < 0.0001$) lower copy number in the

skin compared to other groups, indicating that PM-MCS-dex-NPs formulation reduced the copy number in parallel with the lesion size reduction. Also, copy numbers of G6 and G7 were (9080 ± 5065) and (4704 ± 2755), respectively with significant difference ($p < 0.05$). On the other hand, copy numbers of G5, G6 and G7 were significantly ($p < 0.05$) different with G1 and G11 groups. Comparison of copy numbers in 11 groups one week after treatment are shown in (Fig. 4).

Discussion

Development of a biocompatible polymer formulations provide a new approach to improve leishmaniasis treatment. In this regard, the preparation of polymeric nanoparticles with high drug loading, which would protect the drugs against chemical degradation, and enhance the physical stabilization of the drugs is urgent. Natural protein polymers such as albumin, gelatin and polysaccharides including chitosan, alginate, and starch, have also been reported for their potential to deliver particle-based antileishmanial drugs (Bruni et al., 2017).

Among the various natural polymers, chitosan biopolymer has been widely employed for the formulation of drugs. Chitosan is a natural cationic polysaccharide, with an excellent antibacterial property against various bacteria, viruses, and fungi (Gutha et al., 2017) and exhibits interesting properties, such as bioadhesion, biocompatible and wound-healing properties. Also, chitosan is potent macrophages activators, inducing the release of a range of cytokines and cytotoxic agents. (Bruni et al., 2017). Besides, cationic charge of paromomycin can be masked by complexing it with dextran sulphate polyanion in order to facilitate its incorporation into cationic chitosan nanoparticles. On the other hand, mannose polysaccharide receptor present on the surface of kupffer cells recognize corresponding sugars and facilitate cellular uptake of drug-encapsulated particles. Consequent internalization of the therapeutic carrier facilitates drug accumulation at sites of active parasitic infection (Shahnaz et al., 2017). Mannosylation of drugs largely limits the drug accumulation in macrophage rich organs, and reduce the toxicity in other tissues and organs (Harvier et al., 1995). Thus, for increasing the intracellular accumulation and therapeutic efficacy of PM, we combined paromomycin, chitosan, dextran sulphate and mannose properties for preparing PM-MCS-dex-NPs using ionic gelation method. Various cross-linking methods are available for the development of natural or synthetic polymer based hydrogel, but ionic gelation (polyelectrolyte complexation) by tripolyphosphate (TPP) polyanion as crosslinker is a simple, mild and cost effective technique (Ahirrao et al., 2014).

In vitro results in our previous work (Esfandiari et al., 2019) showed PM-MCS-dex-NPs to be effective in reducing *L. major* amastigotes inside macrophages and in decreasing the cell viability of promastigotes.

Based on our *in vivo* results, superior efficacy of all PM formulation (G2, G3, G4, G5, G6 and G7), compared with free PM was evident. This implies that cationic nature of chitosan facilitates the nanoparticle interaction with negatively charged cell membrane and enhances the endocytosis uptake. It has been reported that the chitosan polymer has the capability to cause a proinflammatory response

such as nitric oxide production by phagocytes which could lead to parasiticidal activity (Shahnaz et al., 2017).

Furthermore, acceleration in lesion size reduction in G7 more than other groups points out the significance of chitosan mannosylation in PM-MCS-NPs. This promoted high drug concentrations intracellularly (macrophage) where *Leishmania* is residing. In agreement with our study, mannose as a macrophage targeting ligand, has been utilized for leishmaniasis treatment with different drugs including doxorubicin (Kole et al., 1999), rifampicin (Chaubey and Mishra., 2014), curcumin (Chaubey et al., 2014), Am B (Vaghela et al., 2018), andrographolide (Sinha et al., 2011), and Bz2MT81 (Mitra et al., 2005). Mannosylated nanoparticles are proved more effective than nonmannosylated nanoparticles and free drugs. Since half-life of PM is 2–3 hours, twice daily dosing of PM-MCS-NPs is acceptable as the total daily dose. Also, this regimen may be useful in mice which cannot tolerate a higher once daily dose to the target daily dose of 20mgkg^{-1} .

On the other hand, based on our findings, G8 and G9, compared to G10, have a significant ($p < 0.05$) effect on wound healing of the mice. The wound healing property of chitosan can be due to various reasons. In this regard, Mehrizi et al., stated that enhancing vascularization and the supply of chito-oligomers at the lesion site can cause better collagen fibril incorporation into the extracellular matrix in leishmaniasis (Mehrizi et al., 2018). Also, administration of chitosan to treat wound infections through mechanisms such as reduction of TNF- α mRNA expression and induction of VEGF production by macrophages has been reported in several studies. Several factors such as molecular weight and the deacetylation degree (DDA) have been suggested to play role in chitosan effect on macrophages (Espuelas et al., 2015; Goy et al., 2009). In the current study, we used a chitosan with moderate weight and height DDA (Q 98%), which is stronger than small chitosan or their oligomers, as reported previously.

No bacterial infection was observed during treatment of G8 and G9, which can be related to excellent antibacterial property of chitosan against various bacteria, viruses, and fungi (Gutha et al., 2017). Antibacterial mechanisms of chitosan can be explained through cell membrane leakage, inhibition of the mRNA, and protein synthesis and suppression of essential nutrients for microbial growth (Goy et al., 2009).

PM is a highly hydrophilic and lipid insoluble drug. At physiological pH, paromomycin is polarized, which limits its distribution in the intracellular fluids and tissues (Kip et al., 2018). To address this concern, PM was encapsulated with mannosylated chitosan. Based on the findings from our previous study (Esfandiari., 2019), PM-MCS-dex-NPs had higher release rate in acidic pH that makes it fit for phagolysosomal environment (pH = 4.5–5.0) of macrophage. On the other hand, there was no evidence for drug accumulation or induction of metabolism upon multiple dosing of PM (Kip et al., 2018). Based on the *in vivo* results, difference between G4, G5, G6, G7 and G1 was significant that is indicative of PM accumulation in macrophages. The superiority of G7 over glucantim and over free PM proves the adequacy of PM-MCS-dex-NPs as the superior drug delivery system for the treatment of intracellular

infections. This study revealed that twice daily PM-MCS-dex-NPs administration had significant efficacy against *leishmania*.

Conclusion

Mannosylation of PM aiming to target macrophage led to the significant antileishmanial activity in *L. major* infected BALB/c mice model. The activity of the IM administration of PM-MCS-dex-NPs was superior to free PM. The promising results supports a novel and effective strategy for treating CL. Considering the significant reduction in lesion size and the parasite DNA copy number, histopathology investigation and bioavailability tests in animals will be required to support the findings and to check the applicability in humans.

Declarations

Conflict of interest

There is no conflict of interest related to this article.

Acknowledgments

The results presented in this research were extracted from Farideh Esfandiari's PhD. dissertation supported by the Research Council of Shiraz University of Medical Sciences (13190). The authors wish to thank Mr. Argasi at the Research Consultation Center (RCC) of Shiraz University of Medical Sciences for his invaluable assistance in editing the paper.

Availability of data and materials

All data generated during this study are included in this published article manuscript and its additional files.

References

1. Ahirrao, S. P., Gide, P. S., Shrivastav, B., Sharma, P. 2014. Ionotropic gelation: a promising cross linking technique for hydrogels. Res. Rev. J. Pharm. Nanotechnol. 2, 1-6.
2. Alvar, J., Velez, I.D., Bern, C., Herrero, M., Desjeux, P., Cano, J., Jannin, J., den Boer, M., 2012. WHO Leishmaniasis control team. Leishmaniasis worldwide and global estimates of its incidence. PLoS One. 7, e35671.
3. Al-Natour, SH., 2009. Update in the treatment of cutaneous leishmaniasis. J. Family. Community. Med. 2009; 16, 41-47.
4. Bavarsad, N., Fazly Bazzaz, B.S., Khamesipour, A., Jaafari, M.R., 2012. Colloidal, *in vitro* and *in vivo* anti-leishmanial properties of transfersomes containing paromomycin sulfate in susceptible BALB/c mice. Acta Trop. 124, 33-41.

5. Bocxlaer, K.V., Caridha, D., Black, C., Vesely, B., Leed S., Sciotti, R.J., Wijnant, G.J., Yardley, V., Braillard, S., Mowbray, C.E., Ioset, J.R., Croft, S.L., in press. Novel benzoxaborole, nitroimidazole and aminopyrazoles with activity against experimental cutaneous leishmaniasis. *Int. J. Parasitol. Drugs. Drug. Resist.* doi: 10.1016/j.ijpddr.2019.02.002.
6. Bruges, A.P., Naveros, B.C., Calpena Campmany, A.C., Pastor, P.H., Saladrigas, R.F., Lizandra, C.R., 2015. Developing cutaneous applications of paromomycin entrapped in stimuli-sensitive block copolymer nanogel dispersions. *Nanomedicine (Lond)*. 10, 227-240.
7. Bruni, N., Stella, B., Giraudo, L., Pepa, C.D., Gastaldi, D., Dosio, F., 2017. Nanostructured delivery systems with improved leishmanicidal activity: a critical review. *Int. J. Nanomedicine*. 12, 5289–5311.
8. Carneiro, G., Santos, D.C.M., Oliveira, M.C., Fernandes, A.P., Ferreira, L.S., Ramaldes, G.A., Nunan, E.A., Ferreira, L.A.M., 2010. Topical delivery and *in vivo* antileishmanial activity of paromomycin-loaded liposomes for treatment of cutaneous leishmaniasis. *J. Liposome. Res.* 20, 16–23.
9. Chellat, F., Merhi, Y., Moreau, A., Yahia, L., 2005. Therapeutic potential of nanoparticulate systems for macrophage targeting. *Biomaterials*. 26, 7260-7275.
10. Chaubey, P., Mishra, B., 2014. Mannose-conjugated chitosan nanoparticles loaded with rifampicin for the treatment of visceral leishmaniasis. *Carbohydr. Polym.* 110, 1101- 1108.
11. Chaubey, P., Patel, R.R., Mishra, B., 2014. Development and optimization of curcumin-loaded mannosylated chitosan nanoparticles using response surface methodology in the treatment of visceral leishmaniasis. *Expert. Opin. Drug. Deliv.* 11, 1-19.
12. Chawla, B., Jhingran, A., Panigrahi, A., Stuart, K.D., Madhubala, R., 2011. Paromomycin affects translation and vesicle-mediated trafficking as revealed by proteomics of paromomycin -susceptible -resistant *Leishmania donovani*. *PLoS One*. 6, e26660.
13. Croft, S. L., Yardley, V., 2002. Chemotherapy of leishmaniasis. *Curr. Pharm.* 8, 319-342.
14. Croft, S.L., Sundar, S., Fairlamb, A.H., 2006. Drug resistance in leishmaniasis. *Clin. Microbiol. Rev.* 9, 111–126.
15. Eddaikra, N., Ait-Oudhia, K., Kherrachi, I., Oury, B., Moulti-Mati, F., Benikhlef, R., Harrat, Z., Sereno, D., 2018. Antimony susceptibility of *Leishmania* isolates collected over a 30-year period in Algeria. *PLoS. Negl. Trop. Dis.* 12, e0006310.
16. Esfandiari, F., Motazedian, M.H., Asgari, Q., Morowvat, M.H., Molaei, M., Heli, H., 2019. Paromomycin-loaded mannosylated chitosan nanoparticles: Synthesis, characterization and targeted drug delivery against leishmaniasis. *Acta Trop.* 31, 105045.
17. Espuelas, S., Irache, J. M., Sanmartin-Grijalba, C., Font, M., Conde, I., Larrea, E., Schwartz, J., Moreno-Amatria, E. 2015. Assessment of β -lapachone loaded in lecithin-chitosan nanoparticles for the topical treatment of cutaneous leishmaniasis in *L. major* infected BALB/c mice. *Nanomedicine*. 11, 2003-2012.
18. Ferreira, L.S., Ramaldes, G.A., Nunan, E.A., Ferreira, L.A., 2004. *In vitro* skin permeation and retention of paromomycin from liposomes for topical treatment of the cutaneous leishmaniasis. *Drug. Dev.*

Ind. Pharm. 30, 289-296.

19. Ghadiri, M., Vatanara, A., Doroud D., Najafabadi, A.R., 2011. Paromomycin loaded solid lipid nanoparticles: Characterization of production parameters. *Biotechnol. Bioproc. E.* 16, 617–623.
20. Goy, R. C., Britto, D. D., & Assis, O. B. (2009). A review of the antimicrobial activity of chitosan. *Polímeros*, 19(3), 241-247.
21. Gutha, Y., Pathak, J.L., Zhang, W., Zhang, Y., Jiao, X., 2017. Antibacterial and wound healing properties of chitosan/poly (vinyl alcohol)/zinc oxide beads (CS/PVA/ZnO). *Int. J. Biol. Macromol.* 103:234-241.
22. Gomez Perez, V., Garcia-Hernandez, R., Corpas-Lopez, V., Tomas, AM., Martin-Sanchez, J., Castanys, S., Gamarro, F., 2016. Decreased antimony uptake and overexpression of genes of thiol metabolism are associated with drug resistance in a canine isolate of *L.infantum*. *Int. J. Parasitol. Drugs. Drug. Resist.* 6,133-139.
23. Harvier, P., Desormeaux, A., Gagne, N., Tremblay, M., Poulin, L., Beauchamp, D., Bergeron, M.G., 1995. Lymphoid tissues targeting of liposome-encapsulated 2', 3'-dideoxyinosine. *AIDS.* 9, 701-707.
24. Jaafari, M.R., Bavarsad, N., Bazzaz, B.S., Samiei, A., Soroush, D., Ghorbani, S., Heravi, M.M., Khamesipour, A., 2009. Effect of topical liposomes containing paromomycin sulfate in the course of *L. major* Infection in susceptible BALB/c Mice). *Antimicrob. Agents. Chemother.* 53, 2259-65.
25. Jhingran, A., Chawla, B., Saxena, S., Barrett, M. P., Madhubala, R. 2009. Paromomycin: uptake and resistance in *Leishmania donovani*. *Molecular and biochemical parasitology.* 164, 111-117.
26. Kalantari, H., Hemmati, A.A., Bavarsad, N., Rezaie, A., Ahmadi, S., 2014. Effect of topical nanoliposomes of paromomycin on rat's liver and kidney. *Jundishapur. J. Nat. Pharm. Prod.* 9, e17565.
27. Kedzierski, L., Sakthianandeswaren, A., Curtis, J.M., Andrews, P.C., Junk, P.C., Kedzierska, K., 2009. Leishmaniasis: current treatment and prospects for new drugs and vaccines. *Curr. Med. Chem.* 16, 599-614.
28. Khadir, F., Shaler, C.R., Oryan, A., Rudak, P.T., Mazzuca, D.M., Taheri, T., Dikeakos, J.D., Haeryfar, S.M.M., Rafati, S., 2018. Therapeutic control of leishmaniasis by inhibitors of the mammalian target of rapamycin. *PLoS. Negl. Trop. Dis.* 12, e0006701.
29. Kip, A. E., Schellens, J. H., Beijnen, J. H., Dorlo, T. P., 2018. Clinical pharmacokinetics of systemically administered antileishmanial drugs. *Clinical pharmacokinetics.* 57, 151-176.
30. Kole, L., Das, L., Das, P.K., 1999. Synergistic effect of interferon-gamma and mannosylated liposome-incorporated doxorubicin in the therapy of experimental visceral leishmaniasis. *J. Infect. Dis.* 180, 811-820.
31. Maarouf, M., Lawrence, F., Croft, S. L., Robert-Gero, M., 1995. Ribosomes of *Leishmania* are a target for the aminoglycosides. *Parasitology research*, 81, 421-425.
32. Mehrizi, T.Z., Ardestani, M.S., Khamesipour, A., Hoseini, M.H.M., Mosaffa, N., Anissian, A., Ramezani, A., 2018. Reduction toxicity of Amphotericin B through loading into a novel nanoformulation of

- anionic linear globular dendrimer for improve treatment of *L. major*. J. Mater. Sci. Mater. Med. 29,125.
33. Mitra, M., Mandal, A.K., Chatterjee, T.K., Das, N., 2005. Targeting of mannosylated liposome incorporated benzyl derivative of *Penicillium nigricans* derived compound MT81 to reticuloendothelial systems for the treatment of visceral leishmaniasis. J. Drug. Target. 13, 285-293.
 34. Mohapatra, S., 2014. Drug resistance in leishmaniasis: Newer developments. Trop. Parasitolol. 4, 4-9.
 35. Ponte-Sucre A, Gamarro F, Dujardin, J.C., Barrett, M.P., López-Vélez, R., Garcia-Hernandez, R., Pountain, A.W., Mwenechanya, R., Papadopoulou, B., 2017. Drug resistance and treatment failure in leishmaniasis: A 21st century challenge. PLoS. Negl. Trop. Dis. 11, e0006052.
 36. Savioli, and L., Daumeric, D., 2010. Organization WH. First WHO report on neglected tropical diseases: Working to overcome the global impact of neglected tropical diseases. 2010, 1-184.
 37. Shahnaz, G., Edagwa, B. J., McMillan, J., Akhtar, S., Raza, A., Qureshi, N. A., Yasinza, M., Gendelman, H. E., 2017. Development of mannose-anchored thiolated amphotericin B nanocarriers for treatment of visceral leishmaniasis. Nanomedicine, 12, 99-115.
 38. Shakibapour, M., Mahmoodi, M., Ghaffari Hoseini, S., Rostami, F., Mansurian, M., Jafari, R., Izadi, S., Charehdar, S., Hejazi, S.H., 2015. Therapeutic effect of acupuncture in BALB/c model of cutaneous leishmaniasis. Adv. Biomed. Res. 4, 1-5.
 39. Shalev, M., Rozenberg, H., Smolkin, B., Nasereddin, A., Kopelyanskiy, D., Belakhov, V., Schrepfer, T., Schacht, J., Jaffe, C.L., Adir, N., Baasov, T., 2015. Structural basis for selective targeting of leishmanial ribosomes: aminoglycoside derivatives as promising therapeutics. Nucleic. Acids. Res. 43, 8601-8613.
 40. Sinha, P.K., Jha, T.K., Thakur, C.P., Nath, D., Mukherjee, S., Aditya, A.K., Sundar, S., 2011. Phase 4 pharmacovigilance trial of paromomycin injection for the treatment of visceral leishmaniasis in India. J. Trop. Med. 2011, 1-7.
 41. Sundar, S., Chakravarty, J., 2008. Paromomycin in the treatment of leishmaniasis. Expert. Opin. Investig. Drugs. 17, 787-794.
 42. Torres-Guerrero, E., Quintanilla-Cedillo, M.R., Ruiz-Esmenjaud, J., Aren, R., 2017. Leishmaniasis: a review. F1000Res. 6, 750.
 43. Vaghela, R., Kulkarni, P.K., Osmani, R.A.M., Varma, V.N.S.K., Bhosale, R.R., Raizaday, A., Hani, U., 2018. Design, development and evaluation of mannosylated oral Amphotericin B nanoparticles for anti-leishmanial therapy: Oral kinetics and macrophage uptake studies. J. Drug. Deliv. Sci. 43, 283-294.
 44. Yasinzai, M., Khan, M., Nadhman, A., Shahnaz, G., 2013. Drug resistance in leishmaniasis: current drug-delivery systems and future perspectives. Future. Med. Chem. 5, 1877-1888.

Tables

Table 2 is not available with this version.

Figures

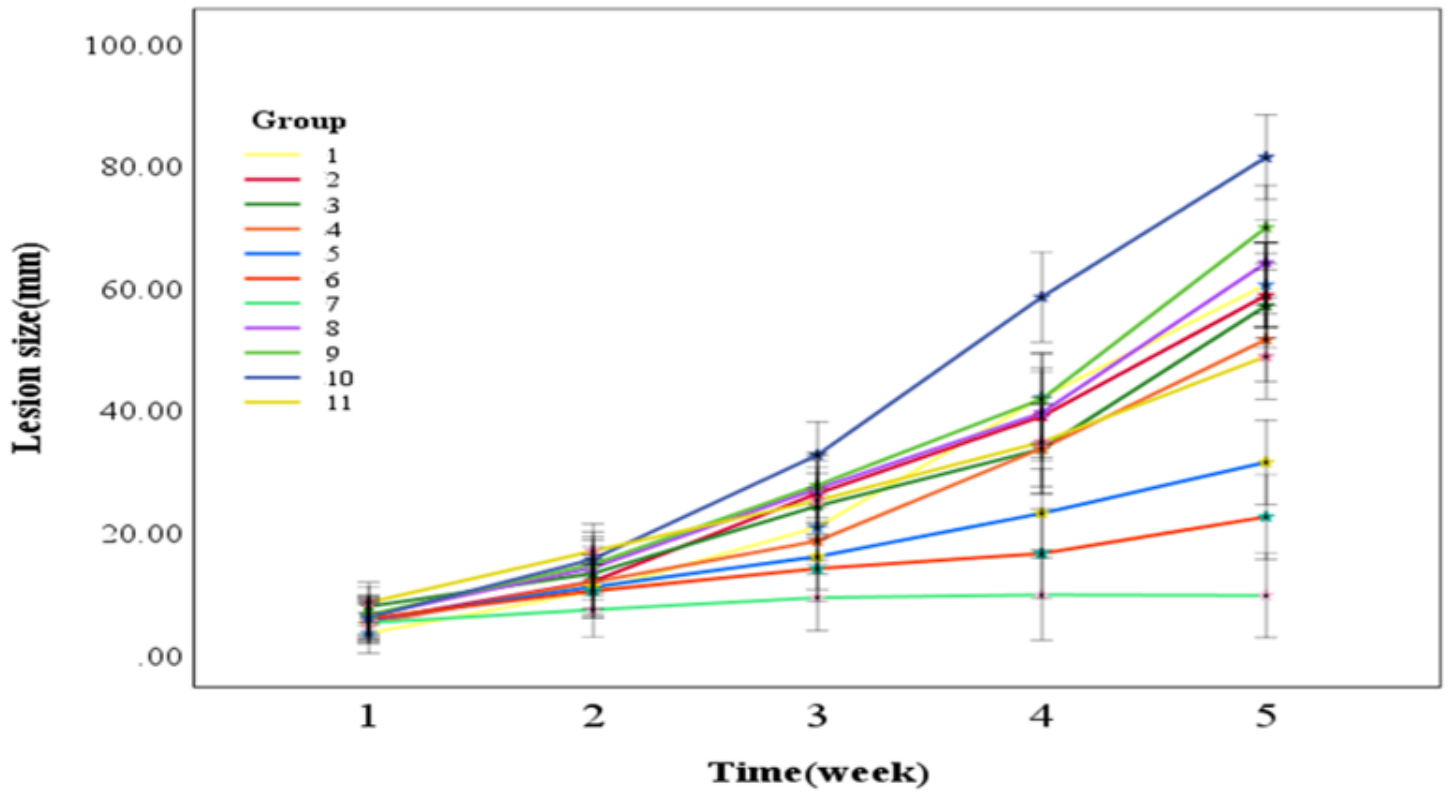


Figure 1

Comparison of lesion size changes during five measuring times in 11 groups.

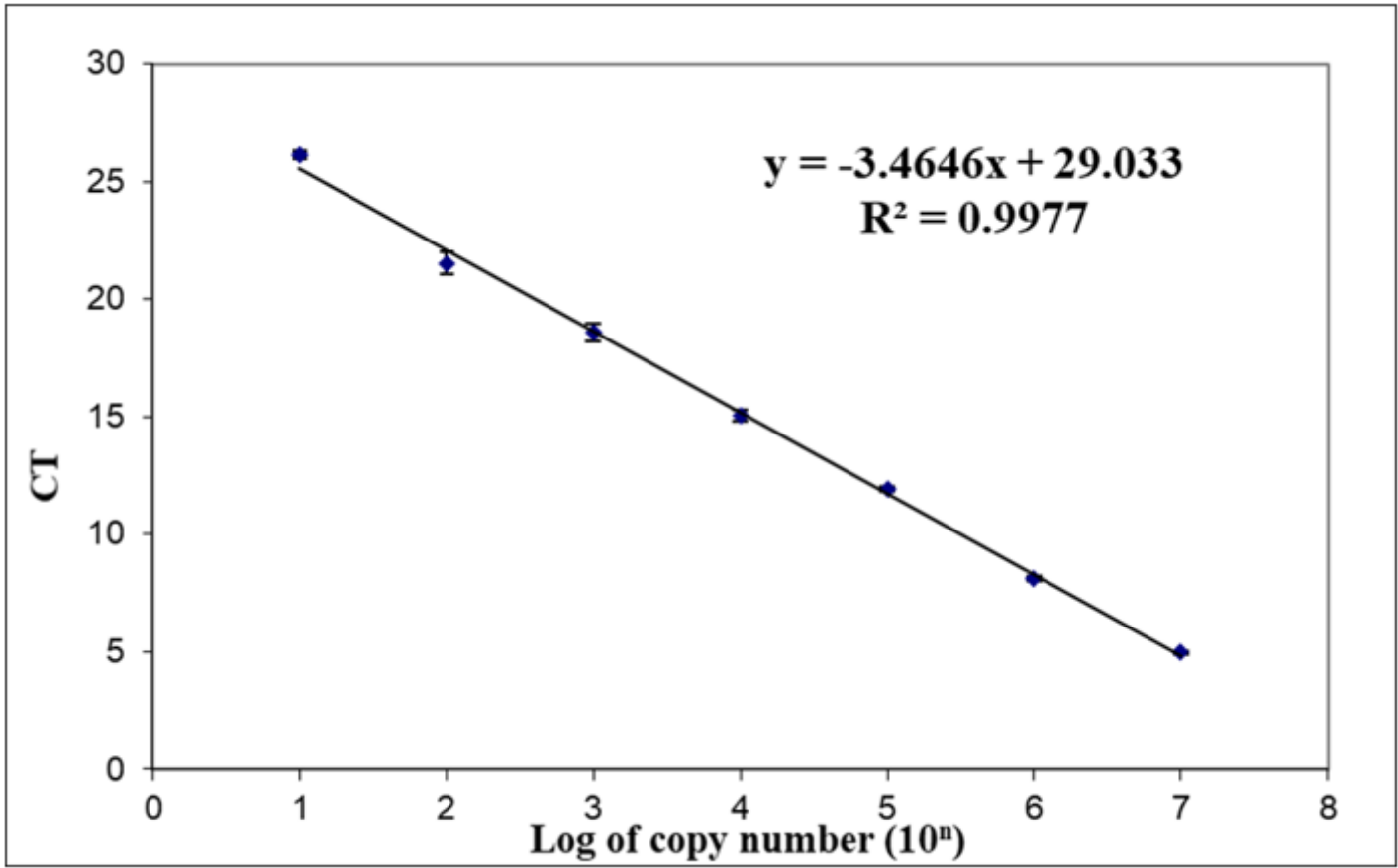


Figure 2

qPCR standard curve for quantification of Leishmania parasite.

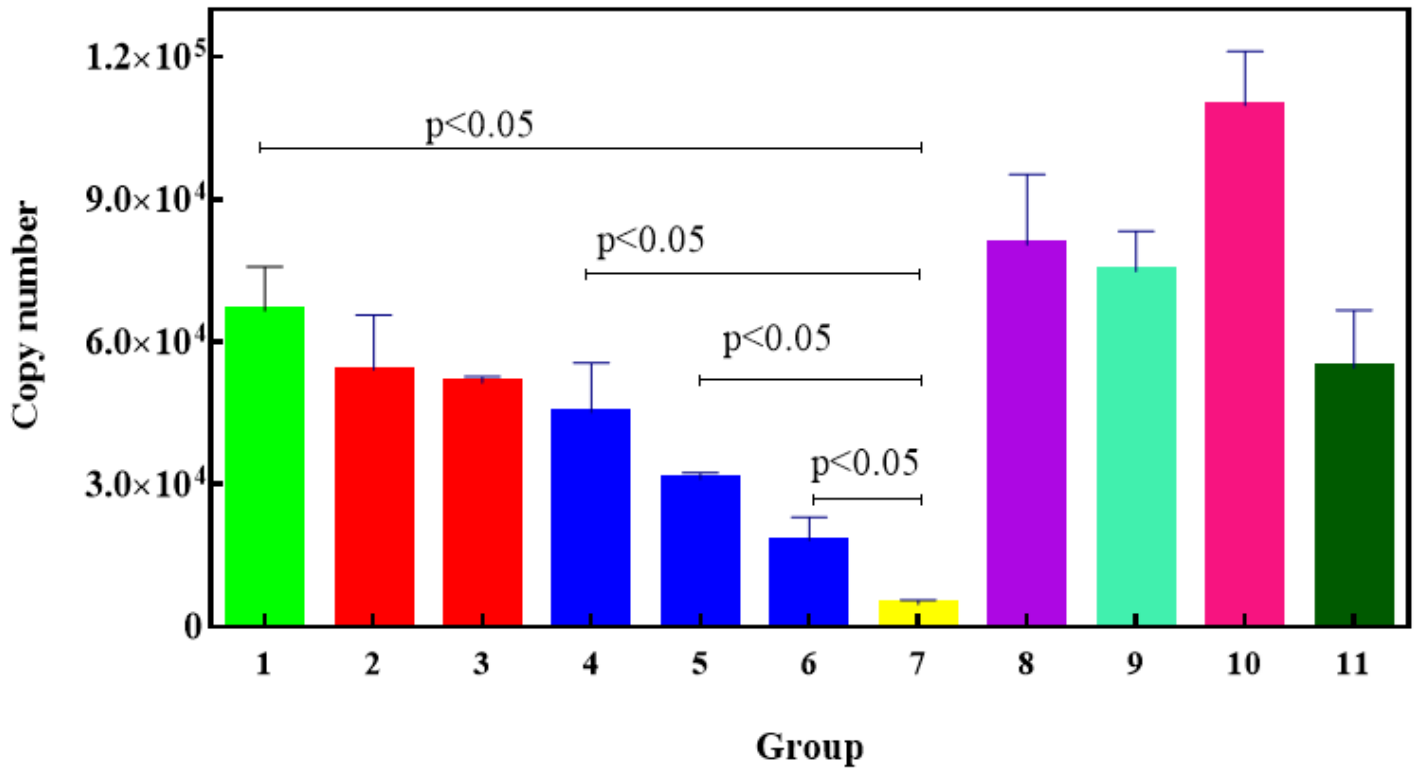


Figure 3

Comparison of the mean \pm SD of copy numbers in all groups one week after completed treatment.

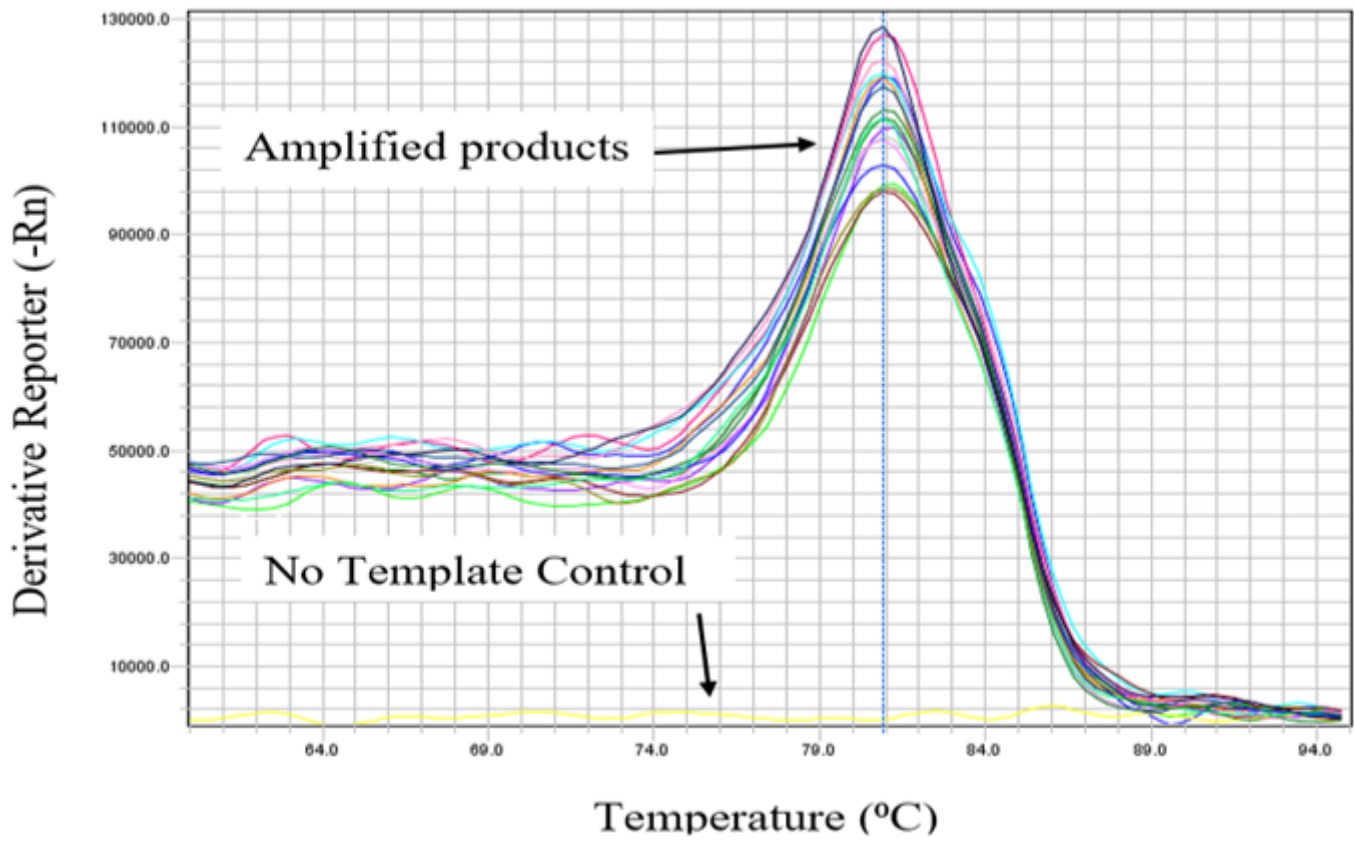


Figure 4

Melting curve of SYBR green qPCR products